

실제모양의 압출기내에서 3차원 유동의 변형특성

김명호^{***}, 김시조^{*}, 임경훈^{*}, 황옥렬^{**}, 김현칠^{***}, 금종구^{***}
^{*}안동대학교 기계공학부, ^{**}경상대학교 기계항공공학부
^{***}(주)LG 화학/테크 센타

Deformation characteristics of three-dimensional flows for the real screw extruder

Myung-Ho Kim^{***}, See-Jo Kim^{*}, Kung-Hun Lim^{*}, Wook-Ryol Hwang^{**},
 Hyun-Chil Kim^{***}, Chong-Ku Kum^{***}

^{*}School of Mech. Eng., Andong National Univ.

^{**}School of Mech. & Aerospace Eng., Kyeongsang National Univ.

^{***}LG Chemical Ltd./Technology Center

Introduction

In the case of single-screw extruders there is a considerable amount of literature on analytical, experimental, and numerical studies about this relationship. In our previous papers[1,3] we have described the basic mixing mechanism of the chaotic mixing to enhance the DC with experimental and numerical approaches. In the case of laminar mixing as the conventional extruder channel flow in the real single-screw extruder it is still valuable to study the actual RTD and DC in order to understand the difference between the quasi-three-dimensional geometry (i.e., the unwound channel geometry) and with the real three-dimensional geometry of the extruder.

Governing equations and numerical methods

The set of equations for the generalized Newtonian fluid is given by.

$$\begin{aligned} \nabla \cdot u = 0, \quad \nabla \cdot \sigma = 0, \quad \text{in } \Omega \\ \sigma = -pI + 2\eta_s D, \quad \text{in } \Omega \end{aligned} \quad \eta(\dot{\gamma}) = \eta_0 / (1 + C \dot{\gamma})^{1-n}$$

The above equations represent the continuity, the momentum balance, and the constitutive relation of the generalized Newtonian fluid, respectively. σ , u , p , D , I , and η_s are the stress, the velocity, the pressure, the rate of deformation tensor, the identity tensor, and the viscosity, respectively. For the generalized Newtonian fluid we use the modified Cross model as a viscosity function with $\eta_0 = 0.1165$, $C = 0.0728$, $n = 0.8389$ (MKS in Unit).

In the down-channel direction, we impose the periodic boundary condition to keep the continuity for both inlet and outlet boundaries for the velocities. In the weak formulation, these periodic boundary conditions are combined with the Lagrangian multipliers together with including the pressure gradient term. We added the additional forcing vector due to the pressure gradient on the inlet boundary.

Particle tracking, evolution of deformation gradient tensor, and DC

In order to analyze RTD and DC of real three-dimensional flow behavior, it is important to understand the trajectories of fluid particles in the real screw extruder channel. The motion of a fluid particle and its evolution of the deformation gradient tensor and the Green deformation tensor can be summarized as follows:

- Considering a solution, ϕ , of the following equation

$$\vec{x} = f(\vec{x}) \text{ with } \vec{x}(0) = \vec{X}$$
- Then, the basic equation of flows and deformations are:

$$\dot{\phi}(\vec{X}) = f(\phi(\vec{X}))$$

$$\dot{\mathbf{F}}(\vec{X}) = \mathbf{L}(\phi(\vec{X})) \cdot \mathbf{F}(\vec{X}) \text{ with } \mathbf{F}_0(\vec{X}) = \mathbf{I}$$

$$\delta \vec{x} = \mathbf{F}(\vec{X}) \cdot \delta \vec{X}$$

$$\mathbf{C}(\phi(\vec{X})) = \mathbf{F}^T(\vec{X}) \cdot \mathbf{F}(\vec{X}) \quad (\delta \vec{x})^2 = \delta \vec{X} \cdot \mathbf{C} \cdot \delta \vec{X}$$
- where \mathbf{F} , \mathbf{L} , and \mathbf{C} are the deformation gradient, velocity gradient and the Green deformation tensor, respectively.

To analyze the deformation process, one first has to obtain the velocity field, which could be determined by the direct numerical simulation using a FEM. Once the real three-dimensional velocity field is known, the particle trajectory and the history of the deformation gradient tensor can be obtained by the forth-order Runge-Kutta method, for example, for the deformation gradient tensor as:

$$\Delta F_y^n = \frac{1}{6}(\Delta t)\{\dot{F}_y^{(0)} + 2(\dot{F}_y^{(1)} + \dot{F}_y^{(2)}) + \dot{F}_y^{(3)}\}$$

$$\therefore F_y^{n+1} = F_y^n + \Delta F_y^n$$

Then the measure of strain as a deformation characteristics is the length stretch, which is defined as[4-7]:

$$\lambda = \underline{\underline{C}} : \underline{\underline{M}} \underline{\underline{M}} = \begin{pmatrix} n_x & n_y & n_z \end{pmatrix} \begin{bmatrix} C_{11} & C_{12} & C_{13} \\ C_{21} & C_{22} & C_{23} \\ C_{31} & C_{32} & C_{33} \end{bmatrix} \begin{Bmatrix} n_x \\ n_y \\ n_z \end{Bmatrix}$$

It might be mentioned that the length stretch is the function of the initial orientation of the material vectors. However, in the single-screw extrusion process, all material vectors aligned with the stream lines have no significant strain during one circulation on the cross-channel of the extruder [4-6]. Therefore, in the previous paper[5], we proposed the modified DC as a new deformation measure for three dimensional flows in extrusion. In this research we investigate the deformation of material vectors perpendicular to the stream line on the cross-sectional domain.

Numerical results and discussion

The geometry of the real single-screw extruder is shown in Fig.2. In this geometry, radius of the barrel, pitch, flight width, and the flight

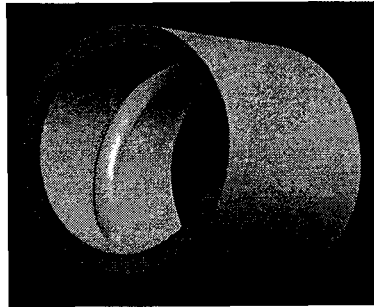


Fig. 2. The geometry of the real single-screw

depth are 45(mm), 45(mm), 5(mm), and 3.7(mm), respectively, and the pressure difference is 3.6588E06(Pa).

As described earlier, the fourth order Runge-Kutta method was used for fluid particle tracking based on the velocity field by the finite-element analysis with applying the periodic boundary condition along the down channel direction.

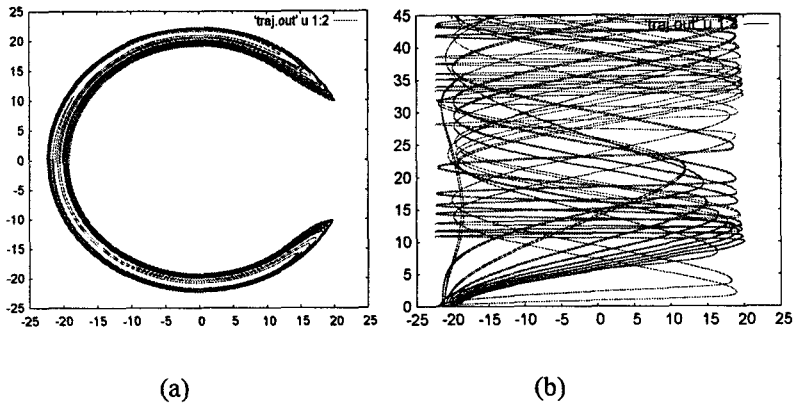


Fig. 3. Particle trajectories in the real screw extruder: (a) 2D plot projected in the cross-sectional plane, (b) in the down-channel direction.

The typical trajectories of fluid particles starting from different positions in the direction of the screw depth as shown in Fig.3. Fig. 3(a) was obtained by rotating the helix angle to the initial cross-sectional plane in order to view the circulatory motion of fluid particles. It is confirmed that trajectories as shown in the cross-sectional plane form closed orbits. Fig. 3(b) shows the fluid particle motion along the down-channel direction.

Fig. 4. shows the distribution of the logarithmic value of the length stretch initially located normal to the stream line on the cross-sectional plane according to the down-channel direction(Z). As shown in Fig. 4, one can clearly see that the local values of the length stretch is increasing as the material vectors go to the down-channel direction. When we consider the RTD, as discussed earlier, as a weighting value in the single-screw extrusion process, we can get the averaged mixing measure along the down channel direction, which will be studied in detail

for the further study. It might be mentioned that there are many numerical troubles to accurately obtain the particle trajectories and the deformation gradient tensor, especially the sub-region where the flight and barrel meet in the real three-dimensional flow fields.

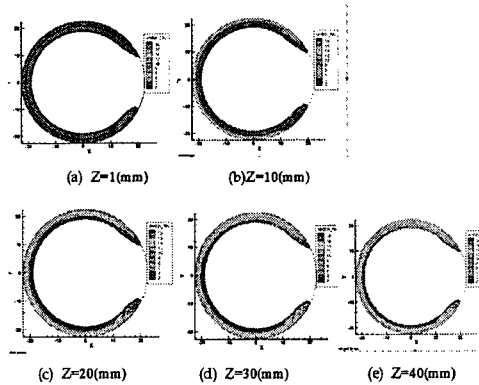


Fig. 4. The distribution of the logarithmic value of the length stretch initially located normal to the stream line on the cross-sectional plane according to the down-channel direction(Z).

Acknowledgements

This work has been supported by the LG Chemical Ltd./Technology Center.

References

- [1] S.J. Kim and T.H. Kwon, *Advances in Polymer Technology*, **15**(1), 55 (1996).
- [2] S.J. Kim and T.H. Kwon, *Powder Technology*, **85**, 227-239 (1995).
- [3] S.J. Kim and T.H. Kwon, *Advances in Polymer Technology*, **15**(1), 41 (1996).
- [4] S.J. Kim and T.H. Kwon, *Polym. Eng. Sci.*, **36**(11), 1454(1996).
- [5] S.J. Kim and T.H. Kwon, *Polym. Eng. Sci.*, **36** (11), 1466, 1996.
- [6] T.H. Kwon, J.W. Joo and S.J. Kim, *Polym. Eng. Sci.*, **34** (3), 174 (1994).
- [7] J.M. Ottino, *The kinematics of mixing: stretching, chaos, and transport*, Cambridge Univ. Press, New York, (1989).
- [8] J.W. Joo and T.H. Kwon, *Polym. Eng. Sci.*, **33** (15), 959 (1993).